Published in final edited form as:
J Nucl Med. 2006 January ; 47(1): 130–139.

Imaging Chemically Modified Adenovirus for Targeting Tumors Expressing Integrin $\alpha_v\beta_3$ in Living Mice with Mutant Herpes Simplex Virus Type 1 Thymidine Kinase PET Reporter Gene

Zhengming Xiong, MD, PhD[1,2], **Zhen Cheng, PhD**[1], **Xianzhong Zhang, PhD**[1], **Manish Patel, PhD**[1], **Joseph C. Wu, MD, PhD**[1], **Sanjiv S. Gambhir, MD, PhD**[1], and **Xiaoyuan Chen, PhD**[1]

[1]Molecular Imaging Program at Stanford (MIPS), Departments of Radiology and Bioengineering, Bio-X Program, Stanford University School of Medicine, Stanford, California

[2]Department of Pediatrics, Tongji Medical College, Huazhong University of Science and Technology and Tongji Hospital, Wuhan, China

Abstract

The aim of this study was to change adenovirus tropism by chemical modification of the fiber knobs with PEGylated RGD peptide for targeting integrin $\alpha_v\beta_3$ that is uniquely or highly expressed in tumor cells and neovasculature of tumors of various origins.

Methods—The first generation Ad (Ad) vector, which expresses the herpes simplex virus type 1 mutant thymidine kinase (HSV1-sr39tk) gene under the control of cytomegalovirus (CMV) promoter was conjugated with poly(ethylene glycol) (PEG) or RGD-PEG. The transduction efficiency of Ads (Adtk, PEG-Adtk, and RGD-PEG-Adtk) into different types of cells (293T, MCF7, MDA-MB-435, and U87MG) was analyzed and quantified by thymidine kinase (TK) assay using 8-^{3}H-penciclovir (8-^{3}H-PCV) as substrate. The in vivo infectivity of the Ad vectors after intravenous administration into integrin $\alpha_v\beta_3$–positive U87MG and MDA-MB-435 tumor-bearing athymic nude mice was measured by both noninvasive microPET using 9-[4-^{18}F-fluoro-3-(hydroxymethyl)butyl]guanine (^{18}F-FHBG) as a reporter probe and ex vivo TK assay of the tumor and tissue homogenates.

Results—PEGylation completely abrogated coxsackievirus and adenovirus receptor (CAR)–knob interaction and the infectivity of PEG-Adtk is significantly lower than that of unmodified Adtk in CAR-positive cells. RGD-PEG–modified virus (RGD-PEG-Adtk) had significantly higher infectivity than PEG-Adtk and the extent of increase is related to both CAR and integrin $\alpha_v\beta_3$ expression levels. ^{18}F-FHBG had minimal nonspecific uptake in the liver and tumors that are void of sr39tk. Mice preinjected intravenously with unmodified Adtk resulted in high hepatic uptake and moderate tumor accumulation of the tracer. In contrast, RGD-PEG-Adtk administration resulted in significantly lower liver uptake without compromising the tumor accumulation of ^{18}F-FHBG. Expression of TK in the liver and tumor homogenates corroborated with the magnitude of ^{18}F-FHBG uptake quantified by noninvasive microPET. Analysis of liver and tumor tissue

For correspondence or reprints contact: Xiaoyuan Chen, PhD, Department of Radiology, Stanford University School of Medicine, 1201 Welch Rd., P095, Stanford, CA 94305-5484. shawchen@stanford.edu.

integrin level confirmed that RGD–integrin interaction is responsible for the enhanced tumor infectivity of RGD-PEG-Adtk.

Conclusion—The results of this study suggest that RGD-PEG conjugation is an effective way to modify Ad vector tropism for improved systemic gene delivery. Noninvasive PET and ^{18}F-FHBG are able to monitor in vivo transfectivity of both Adtk and RGD-PEG-Adtk vectors in the liver and tumors after intravenous injection.

Keywords

adenovirus; reporter gene; gene therapy; integrin; RGD; PET

Recombinant adenovirus (rAd) has been widely used as an attractive gene delivery vehicle to mammalian cells because of its unparalleled efficacy in accomplishing gene transfer in vivo (1,2). There are, however, some limitations associated with Ad for gene delivery. One such disadvantage is related to the wide native tropism of Ad, which often results in high accumulation in nontargeting tissues (3–9). Another major disadvantage for using Ad vector in vivo is that administration of Ad to a host leads to the host immune response against Ad (10–12). Vector targeting to a specific tissue of cell type would enhance gene therapy efficacy and permit the delivery of lower doses, which would consequently result in reduced toxicity.

Cell-specific gene delivery via Ad vectors has been achieved by both genetic (13–15) and chemical (16–22) approaches. Chemical modification is a nongenetic strategy to modify the surface of a viron by covalently attaching a polymer containing the targeting ligand with the lysine residues on the surface of Ad. Modification of Ad vectors with poly(ethylene glycol) (PEG) prolongs persistence in the blood and circumvents inflammatory and humoral immune responses (16–22). However, the PEGylation of Ad vectors also leads to loss of infectivity due to the steric hindrance induced by PEG chains. To overcome the decreased efficiency of infection of PEGylated Ad, vectors containing functional molecules on the tip of PEG restore target-specific infectivity. Lanciotti et al. reported targeted Ad vectors using heterofunctional PEG and FGF-2 (22). Ogawara et al. (17) reported PEGylated Ad vectors containing E-selectin–specific antibody or α_v integrin–specific RGD peptide for targeting activated endothelial cells. Ad vectors coated with polymers other than PEG have also been developed. Fisher et al. used a multivalent hydrophilic polymer based on poly[*N*-(2-hydroxypropyl) methacrylamide] to modify Ad vectors (23). Although improved pharmacokinetic properties of polymer-coated Ad vectors without ligands have been reported, those of polymer-coated Ad vectors with ligands have not been reported in detail.

Most studies performed in animal models to optimize vector targeting and functional gene delivery use protocols that require the animals to be sacrificed to monitor reporter gene expression. Recently, however, several noninvasive technologies for monitoring reporter gene expression in vivo have been described (24). The most commonly used PET reporter gene is herpes simplex virus 1 thymidine kinase (HSV1-tk). Many of the enzyme substrates have been labeled with ^{18}F or ^{124}I to image HSV1-tk gene expression. Two major substrates for HSV1-tk enzyme/PET include 9-[4-^{18}F-fluoro-3-(hydroxymethyl)butyl]guanine (^{18}F-FHBG) and ^{124}I- or ^{18}F-labeled 2′-fluoro-2′-deoxy-5′-iodo-1-β-D-arabinofuranosyluracil

(^{124}I-FIAU or ^{18}F-FIAU) (25–27). It has also been reported that the mutant HSV1-sr39tk is more effective than the wild-type HSV1-tk at using acycloguanosines as substrates. We have demonstrated that the utility of HSV1-sr39tk and ^{18}F-FHBG is able to monitor the reporter gene expression over a 3-mo period after somatic gene transfer (26,28).

In this study, a replication-deficient Ad was modified with bifunctional PEG and then conjugated with cyclic RGD peptide (Fig. 1). We hypothesized that surface modification of Ad fiber knobs with PEGylated-RGD peptide will ablate the normal tropism and reduce transduction of nontarget tissues in vivo; incorporation of integrin $\alpha_v\beta_3$–specific RGD peptides will enhance the gene delivery to tumor neovasculature and integrin-positive tumor cells. To monitor the localization and expression of the chemically modified virus we packed the HSV1-sr39tk mutant as a reporter gene under the control of cytomegalovirus (CMV) promoter. The homing selectivity and transgene expression after intravenous administration of integrin-directed adenovirus were studied by microPET using ^{18}F-FHBG as a reporter probe.

MATERIALS AND METHODS

Materials

All commercially available chemical reagents were used without further purification. Cyclic RGD pentapeptide c(RGDyK) was prepared following a previously reported procedure (29). Introduction of a sulfhydryl group to RGD peptide was realized by reacting the active NHS ester (where NHS = *N*-hydroxysuccinimide) end of *N*-succinimidyl-*S*-acetylthioacetate (SATA) with the available lysine ε-amino group on the RGD peptide to form a stable amide linkage. Deprotection with hydroxylamine of the acetylated thiol of SATA-modified RGD peptide yielded a free sufhydryl group c(RGDy(ε-acetylthiol)K) (RGD-SH). Purification of the crude product was performed on a semipreparative reversed-phase high-performance liquid chromatography (HPLC) system equipped with a 170U 4-channel UV-visible absorbance detector (Dionex Summit HPLC system; Dionex Corp.) using a Vydac protein and peptide column (218TP510; 5 μm, 250 × 10 mm). The flow was 5 mL/min, with the mobile phase starting from 95% solvent A (0.1% trifluoroacetic acid [TFA] in water) and 5% solvent B (0.1% TFA in acetonitrile) (0–3 min) to 35% solvent A and 65% solvent B at 33 min. The analytic HPLC method was performed with the same gradient system, but with a Vydac 218TP54 column (5 μm, 250 × 4.6 mm) and flow rate of 1 mL/min.

Cell Culture

Human breast cancer cell lines MCF-7 and MDA-MB-435, glioblastoma U87MG, and embryonic kidney cells 293T were purchased from the American Type Culture Collection. Cells were cultured at 37°C in a humidified atmosphere containing 5% CO_2 in Iscove's modified Dulbecco medium or Leibovitz's L-medium and 5% fetal bovine serum (FBS) (Life Technologies, Inc.).

Flow Cytometry

Of the 4 cell types used for in vitro transduction studies, the expression levels of integrin $\alpha_v\beta_3$ and coxsackievirus and adenovirus receptor CAR) were determined by flow cytometry.

Cells grown in T75 flasks were harvested by incubation with 0.2% ethylenediaminetetraacetic acid. The cell pellets were resuspended in phosphate-buffered saline (PBS) containing 2% FBS. One million cells were incubated at 4°C for 1 h with the primary antibodies (LM609 for human integrin $\alpha_v\beta_3$ [Chemicon]; H-300 for CAR [Santa Cruz Biotechnology, Inc.]). The cells were washed 3 times, followed by incubation with the secondary antibodies (Alexa488-labeled antimouse IgG for LM609 and antirat IgG for H-300, respectively; Molecular Probes) at 4°C for 1 h. The cells were resuspended in 500 μL of PBS and 30 μL of propidium iodide (Sigma) for flow cytometry analysis (FACScan). Ten thousand events were scored for each cell line. The same secondary antibodies alone served as the negative control for each cell line.

Construction and Purification of Recombinant Adenovirus

Construction of the first-generation Ad vectors that expressed mutant HSV1-sr39tk gene under the control of CMV promoter (Ad-pCMV-sr39tk) were amplified in 293T cells using a modification of established methods (28). Further large-scale amplification and purification were performed by ViraQuest Inc. using the conventional double CsCl gradient-centrifugation method. The number of viral particles (v.p.) was determined by measurement of the optical density of virus at 260 nm (OD_{260}). Determination of virus particle titer was accomplished spectrometrically. The ratio between the v.p. and plaque-forming units (pfu) was found to be 30:1.

Chemical Modification of Adenovirus

The synthetic scheme for preparation of RGD-PEG was shown in Figure 1. The bifunctional PEG (NHS-PEG-MAL, molecular weight = 3,400 Da; Nektar Therapeutics) (20 mg, ~6 μmol) in NaOAc buffer (0.1 mol/L, pH 6.0, 500 μL) was added to RGD-SH (5 mg, ~7 μmol) in dimethyl sulfoxide (DMSO) (40 μL). The reaction mixture was allowed to stand at room temperature for 1 h. An excess amount of RGD was used to ensure the complete consumption of PEG. The bifunctional PEG and RGD-PEG-NHS were used for covalent attachment to Ads. In brief, an aliquot of NHS-PEG-MAL or RGD-PEG-NHS dissolved in DMSO (100 mg/mL) was added slowly to the virus (10^{12} v.p.) in a 10^5 mol:1 mol ratio. The reaction mixture was protected from light and gently stirred for 2 h at 4°C. The excess amount of PEG was removed using a PD-10 column (Amersham Biosciences). The purified vector was stored as stock solution for further in vitro and in vivo assays.

A fluorescamine assay was used to estimate the degree of conjugated ligand on the adenovirus, following the procedure published earlier (16). Briefly, a series of samples (20, 40, 60, 80, and 100 μg/mL) of modified and unmodified viruses (50 μL) were mixed with 50 μL of 0.1 mg/mL fluorescamine (Sigma) in acetone. The reactions were performed in the dark at room temperature for 15 min. The measurement of fluorescence of the samples was then performed using an HTS 7000 Plus plate reader (Perkin–Elmer Inc.), with an excitation wavelength of 390 nm and an emission wavelength of 475 nm. Protein levels of modified and unmodified vectors were determined by a Micro BCA (bicin-choninic acid) assay (Pierce Biotechnologies). The degree of conjugation was determined by comparing the slopes of modified virus with unmodified virus. The percentage of modification was then expressed as $100 \times (1 - \text{slope}_{\text{modified}}/\text{slope}_{\text{unmodified}})$. Bovine serum albumin (BSA) was

used as the standard. The resulting fluorescence is proportional to the concentration of free amino groups on the virus capsid. Standard curves were generated for each time point by plotting protein concentration versus fluorescence units. The degree of modification was obtained as the ratio between the slopes of conjugated and unconjugated viruses at similar time points.

In Vitro Transduction Assay

The assays were performed as described previously (17) with slight modifications. In brief, cells were seeded into 24-well plates (5×10^4 cells/well) and infected 48 h later with 10^3 particles per cell of unmodified virus (Adtk), PEGylated virus (PEG-Adtk), or RGD-PEG–modified virus (RGD-PEG-Adtk) in triplicates in culture medium with 2% FBS and incubated for 4 h at 37°C. The incubation medium was then replaced by normal medium and cells were further incubated for 48 h. Cells were harvested and lysed with 500 μL of TK lysis buffer that contained 0.5% Nonidet P-40 (NP-40; Sigma-Aldrich), 20 mmol/L *N*-(2-hydroxyethyl) piperazine-*N*′-(2-ethanesulfonic acid) (HEPES) (pH 7.6), 2 mmol/L $Mg(OAc)_2$, 1 mmol/L dithiothreitol, and 50 μmol/L thymidine (30). The supernatant was collected after centrifugation. The samples were kept at −80°C until use. The modified and unmodified adenovirus protein concentrations were determined by the Micro BCA assay. One microgram of cell extract was incubated with HSV1-tk substrate 8-^{3}H-penciclovir (8-^{3}H-PCV). The phosphorylated tracer was separated from unphosphorylated 8-^{3}H-PCV with DE-81 filters (Whatman International Ltd.). TK activity is expressed as the percentage of conversion of substrate per minute per microgram protein.

Animal Models

All experimental procedures involving animals were conducted in accordance with the institutional guidelines set forth by Stanford University. Immunodeficient female athymic nude mice were housed in specific pathogen-free facilities. The MDA-MB-435 breast cancer model was established by orthotopic injection of 5×10^6 cells into the left mammary fat pad. The U87MG glio-blastoma model was obtained by injecting a mixture of 5×10^6 cells suspended in 50 μL medium and 50 μL Matrigel (BD Biosciences) into the right front leg of nude mice.

microPET Studies

Recombinant adenoviruses expressing the mutant HSV1-sr39tk from the CMV promoter (Adtk, PEG-Adtk, or RGD-PEG-Adtk) were injected by tail vein into tumor-bearing mice. Each mouse was tail vein injected with 1.25×10^{12} v.p./kg (4.15×10^{10} pfu/kg). Forty-eight hours later, the mice were subjected to imaging studies on a microPET R4 rodent model scanner (Concorde Microsystems Inc.). Mice were injected via tail vein with ^{18}F-FHBG (3.7–7.4 MBq [100–200 μCi]) (28). After 1 h, mice were anesthetized with 2% isoflurane and placed in the prone position and near the center of the field of view of the microPET. The 10-min static scans were obtained and the images were reconstructed by a 2-dimensional ordered-subsets expectation maximum (OSEM) algorithm. The images were then processed for quantitative analysis using ASIpro VM microPET Data Analysis Software (Concorde Microsystems Inc.). Briefly, regions of interest (ROIs) were drawn over

the tumor on decay-corrected, whole-body coronal images. The counts per pixel per minute were obtained from the ROI and converted to counts/mL/min by using a calibration constant. By assuming a tissue density of 1 g/mL, the ROIs were converted to counts/g/min. An image ROI–derived percentage injected dose (ID) per gram of tissue (%ID/g) was then determined by dividing counts/g/min with ID.

Measurement of Transgene Expression and Tissue Integrin Level

After PET, the animals were sacrificed, and the tumors and liver tissues were collected and stored at −80°C until used for the TK assay. About 500 μg of tissue was washed with PBS (twice), homogenized in lysis buffer, incubated for 20 min at room temperature, and then centrifuged at 13,500 rpm for 5 min. Fifty microliters of supernatant were transferred to a new tube and used for the TK and protein assays. TK activity was measured with 8-^{3}H-PCV as substrate and the protein assay was performed using the Micro BCA assay kit.

The quantitation of tissue integrin level was performed by incubating NP-40–solubilized tumor tissue lysate with ^{125}I-echistatin (31) and then quantified by sodium dodecyl sulfate polyacrylamide gel electrophoresis (SDS-PAGE) and autoradiography. Briefly, solubilized tumor and liver tissues were obtained by addition of 0.1 mL/cm^2 of lysis buffer (0.05 mol/L HEPES [pH 7.4], 1% NP-40, 1 mmol/L $CaCl_2$, and 1 mmol/L $MgCl_2$). After being kept on ice for 10–20 min, the samples were collected and centrifuged at 15,000 rpm for 3 min. The resulting solution was then analyzed for total protein content by Micro BCA protein assay. Samples were assayed in triplicate. Twenty micrograms of proteins were incubated in a final volume of 25 μL in binding buffer in the presence of 1.85 kBq of ^{125}I-echistatin. After a 2-h incubation at room temperature, the mixtures were loaded onto a 4%–10% SDS-PAGE gradient gel. After electrophoresis, the gels were dried and subjected to autoradiograghy overnight. Radioactive bands were developed and quantified in a Cyclone PhosphoImager system (Perkin–Elmer Inc.). The same dose of ^{125}I-echistatin without forming complex with integrin was used as a standard and 15 ng of purified integrin $\alpha_v\beta_3$ (Chemicon) was used as a positive control and molecular marker.

Statistical Analysis

Data are expressed as mean ± SD. One-way ANOVA was used for statistical evaluation. Means were compared using the Student *t* test. $P < 0.05$ was considered significant.

RESULTS

Chemistry

The synthetic scheme for NHS-PEG-RGD conjugate is shown in Figure 1. The active NHS end of SATA reacts with the ε-amine group in the cyclic RGD peptide lysine residue to form a stable amide linkage. The completion of the reaction was confirmed by the disappearance of the RGD peptide peak at 10.9 min and the appearance of the SATA conjugate peak at 12.1 min on the analytic HPLC. Deacetylation of SATA with hydroxylamine gives almost quantitative yield of RGD-SH (retention time [t_{Ret}] = 10.6 min). Note that deprotection under neutral condition results in partial oxidation of RGD-SH to RGD-S-S-RGD (t_{Ret} = 13.4 min). The conjugation of bifunctional NHS-PEG-MAL with

RGD-SH was accomplished by reaction of the maleimide of PEG with the free thiol under slightly acidic condition to avoid partial hydrolysis of the NHS ester. The product RGD-PEG-NHS (broad peak at 20.6 min) was well separated from the parent RGD-SH. The broad peak of NHS-PEG-MAL at 21.9 min completely disappeared. The NHS ester of bifunctional PEG under the same condition without adding RGD-SH was stable. The matrix-assisted laser desorption/ionization time-of-flight (MALDI-TOF) mass spectrum gave a group of peaks with the maximum counts at a molecular weight around 4,150 Da. Note that the group of mass spectral peak obtained is attributed to the fact that the PEG linker is a collection of molecules with varying number of ethylene glycol units with an average molecular weight of 3,400 Da. The NHS active ester group of the PEG (either NHS-PEG-MAL or NHS-PEG-RGD) molecule reacts with virus surface lysine amino groups to form a stable amide bond. Using 10^5 PEG per virion, we were able to demonstrate conjugation of about 55%–60% of reactive groups on the viral caspid by a fluorescamine assay. Further increases in PEG concentration do not result in higher conjugation.

Transduction Efficiency of PEGylated Adenoviruses

As shown in Figure 2, all 4 cell types used expressed CAR, in rank order of 293T > U87MG > MCF-7 > MDA-MB-435. Integrin $\alpha_v\beta_3$ was only detectable in U87MG and MDA-MB-435 cells, with U87MG > MDA-MB-435. U87MG, MDA-MB-435, MCF-7, and 293T cells, which exhibit different expression levels in CAR and integrin $\alpha_v\beta_3$ were infected with Adtk, PEG-Adtk, and RGD-PEG-Adtk. For the unmodified Adtk, the infectivity follows the order of 293T ≫ U87MG > MCF-7 > MDA-MB-435, which is consistent with the CAR expression of these cells (Fig. 3). In 293T cells, viral infectivity was almost completely ablated. TK expression of the 60% modified PEG-Adtk was ~200-fold lower than that of unmodified Adtk. The other 3 cell lines also showed significant decreases in infectivity of Adtk on PEGylation ($P < 0.0001$), suggesting that the PEG molecule is shielding the viral knob from recognizing CAR. Enhanced transduction efficiency of RGD-PEG-Adtk was observed as compared with that induced by PEG-Adtk in all 4 cell types. In 293T cells, RGD-PEG-Adtk showed 90-fold higher TK expression than PEG-Adtk, which exhibited the same level of modification. This gene expression level was only slightly lower than that of unmodified Adtk, albeit that 293T cells are integrin negative (Fig. 2C). In MCF-7 cells, infectivity was not affected by RGD modification, presumably due to the fact that this cell line is integrin negative and expresses a low level of CAR. Note that the infectivity of RGD-PEG-Adtk in U87MG cells was only 3-folder higher as compared with that of PEG-Ad. The transduction of RGD-PEG-Adtk was about 5-fold less than that of the unmodified Adtk, indicating that the existence of both CAR and integrin $\alpha_v\beta_3$ together likely facilitate the infectivity of adenovirus.

Monitoring Transgene Expression In Vivo

For each tumor type (U87MG and MDA-MB-435), 3 groups ($n = 3$/group) of mice were studied. The mice without virus administration showed minimal tumor and liver uptake of ^{18}F-FHBG. Prominent activity accumulation in the gallbladder, intestines, and urinary bladder was found at 1 h after injection of 3.7–7.4 MBq (100–200 μCi) of ^{18}F-FHBG, reflecting both hepatobiliary and renal excretion of this compound (Fig. 4). Mice preinjected (48 h before microPET) via the tail vein with unmodified Ad vector Adtk showed a

relatively high hepatic uptake (2.1 ± 0.7 %ID/g) (Fig. 5A). The average ^{18}F-FHBG retention in U87MG and MDA-MB-435 tumors was 0.72 ± 0.27 and 0.81 ± 0.20 %ID/g, respectively. The liver uptake of ^{18}F-FHBG in mice preinjected with RGD-PEG-Adtk (0.33 ± 0.30 %ID/g) is significantly lower than that in mice with unmodified virus ($P < 0.0001$), although this value is higher than that in mice without virus (0.08 ± 0.01 %ID/g). Both Adtk- and RGD-PEG-Adtk–infected mice had significantly higher tumor uptake than mice without virus ($P < 0.001$); however, no difference in tumor accumulation was found between the 2 types of virus-infected mices. For the unmodified Ad vector, significantly higher infectivity in the liver than in the tumors reflect the fact that unmodified virus interacts with tissues through CAR recognition. In contrast, RGD-PEG–modified Ad vector showed a higher infectivity in the tumors than in the liver tissue, which is very likely due to the higher integrin $\alpha_v\beta_3$ expression of U87MG and MDA-MB-435 tumor tissues as compared with liver.

Ex Vivo Measurement of TK

Twelve hours after the microPET study, mice were euthanized and the liver and tumor tissues were dissected for assay of TK activity. The unmodified adenovirus showed significantly higher liver TK expression than that of RGD-PEG-Adtk ($P < 0.0001$), corroborated with what is observed for the liver uptake while imaging with ^{18}F-FHBG. Slightly higher TK activity was detected in both U87MG and MDA-MB-435 tumors infected with RGD-PEG-Adtk as compared with those infected with Adtk, but the difference was not significant (Fig. 5B). Despite the fact that the infectivities of both Adtk and RGD-PEG-Adtk in U87MG cells were significantly higher than those in MDA-MB-435 cells ($P < 0.005$), we did not observe difference in tumor uptake of ^{18}F-FHBG in vivo. No difference in tissue TK enzyme activity was found in these 2 tumor tissue lysates, either. To understand whether the in vivo infectivity is related to tissue and organ integrin expression, we analyzed integrin density in the liver and in U87MG and MDA-MB-435 tumors. As quantified by SDS-PAGE/autoradiography, U87MG and MDA-MB-435 tumors express similar levels of integrins, which is higher than that in the liver (Fig. 6). The receptor-binding assay based on cell and tissue lysates using ^{125}I-echistatin as the radioligand and nonradioactive echistatin as the competitor found that the MDA-MB-435 tumor tissue integrin level (number of receptors/mg protein) is about 4- to 5-fold higher than that of MDA-MB-435 tumor cells. However, no significant difference was found between U87MG tumor cells and U87MG tumor tissue. It is likely that the stromal cells and endothelial cells in MDA-MB-435 tumor express more integrin than those in U87MG. The overall effect is that these 2 tumors have similar integrin density in vivo.

DISCUSSION

The expression of the adhesion molecule integrin $\alpha_v\beta_3$ on sprouting capillary cells and their interaction with specific matrix ligands has been shown to play a key role in tumor angiogenesis and metastasis (32,33). During the last few years, we and others have developed a series of RGD peptide probes for multimodality imaging of tumor integrin expression, including PET, SPECT, and near-infrared fluorescence (34–36). E1- and E-3 deleted adenovirus encoding luciferase as a reporter gene has been modified with RGD-PEG

conjugate and applied the RGD-PEG-AdTL to home into inflamed skin in mice with delayed-type hypersensitivity inflammation, resulting in local expression of the reporter transgene luciferase (17). In this study we followed a similar strategy (17) using HSV1-sr39tk as the reporter gene and used noninvasive PET to monitor RGD-PEG-Adtk–mediated Ad DNA delivery to integrin-positive tumor models. Using PEG-Adtk or RGD-PEG-Adtk in a ratio of 10^5 mol:1 mol PEG:v.p. we were able to demonstrate conjugation of up to 60% of reactive amino groups on the viral caspid by the fluorescamine assay. Further increases in PEG concentration did not result in further conjugation. This level of surface modification was estimated to have about 11,000 PEG molecules attached to the virion assuming a total of 18,000 reactive amine groups on the virus surface (16). The average particle size of Ad was increased with PEGylation; the average particle size of PEG-Adtk and RGD-PEG-Adtk was about 10 nm bigger than that observed in the unmodified Adtk, consistent with previous studies (23). SDS-PAGE analysis also showed the presence of a new band of PEGylated viral caspid protein (data not shown).

In vitro studies in cells with different CAR and integrin expression (Fig. 2) showed that unmodified adenovirus infectivity is well correlated with CAR expression and corroborated with most other reports in the literature that infection of adenovirus is initiated by high-affinity binding of the C-terminal knob part of the fiber protein to CAR receptor. PEGylation almost completely ablated infectivity in CAR-positive cells (such as 293T and U87MG). The difference is less distinct in CAR-negative cells (such as MDA-MB-435), in which α_v integrin and heparan sulfate might be responsible for viral entry into cells, which cannot be blocked by PEGylation. Note that RGD-PEG-Adtk exhibited a relatively high transduction as compared with PEG-Adtk in all 4 cell lines; however, the extent of enhancement in infectivity is not consistent with the cell-surface integrin expression level. The infectivity of RGD-PEG-Adtk in 293T cells with high CAR and low integrin expression is about 90-fold higher than PEG-Adtk, whereas the infectivity of RGD-PEG-Adtk in U87MG cells with high integrin but relatively low CAR expression is only 3- to 4-fold higher than that of PEG-Adtk. These seemingly contradictory results indicate that the existence of both CAR and $\alpha_v\beta_3$ integrin together likely facilitate the infectivity of adenovirus. It is likely that surface modification with PEG-RGD led to the RGD–integrin interaction responsible for both virus attachment (chemical modification by adding RGD to the fiber knob) and internalization (existing RGD peptides in the penton base) (37).

^{18}F-FHBG as a PET reporter probe for HSV1-sr39tk had minimal hepatic and tumor uptake in control mice without adenovirus administration. Similar to what is observed in Swiss Webster mice (28), we observed extensive tracer uptake in the liver after unmodified Adtk vector administration, presumably due to liver tropism of the Ad vectors. PEG-Adtk, with very low infectivity in vitro, also had minimal liver and tumor infectivity. RGD-PEG-Adtk–treated mice had higher liver accumulation of ^{18}F-FHBG than that of PEG-Adtk–treated and untreated mice, this uptake is likely due to combined CAR and integrin recognition, as SDS-PAGE/autoradiography showed that liver tissue has moderate integrin expression (Fig. 6). This is also supported by our previous studies that liver uptake of radiolabeled RGD peptides was effectively blocked by coinjection with unlabeled RGD peptides, demonstrating at least partial integrin specificity of the radiopeptides in addition to the normal hepatic kinetics (29,38). The highest modification rate was reported to be 85% (16).

In our case, we were able to modify 55%–60% of the surface amines with PEG or PEG-RGD (molecular weight of PEG is ~3,400 Da). Due to the steric hindrance of the PEGylation, most of the remaining free amines may have been shielded from coupling with PEG. This at least, in part, explains why PEGylated viral vectors had significantly decreased liver infectivity. The liver infectivity might be a combination of CAR and integrin recognition (Fig. 6 also showed some integrin expression in the liver tissue).

It is interesting that a minimal difference in tumor uptake of ^{18}F-FHBG or TK activity was found between U87MG and MDA-MB-435 tumors infected with RGD-PEG-Adtk in vivo despite the fact that U87MG cells had almost 8-fold higher infectivity than MDA-MB-435 cells transduced with the same vector. Flow cytometry indicated that U87MG cells had 5-fold higher integrin expression than MDA-MB-435, corroborating with receptor density calculated from a whole-cell binding assay using ^{125}I-echistatin as radio-ligand (data not shown). This difference, however, is leveraged in the tumor tissue (Fig. 6). Quantification of receptor density from MDA-MB-435 cell and MDA-MB-435 tumor tissue lysates also showed that the tumor had a significantly higher integrin level than that in the cells normalized to the same amount of protein. The similar tumor uptake of ^{18}F-FHBG and TK activity in both tumor models is thus a reasonable reflection of integrin-specific delivery of RGD-PEG-Adtk. Further confirmation of integrin specificity requires the demonstration of the inability of scrambled RGD peptide-PEG-Adtk to enhance tumor uptake of ^{18}F-FHBG or tumor TK activity measured by the TK assay.

It is also notable that ^{18}F-FHBG had prominent activity accumulation in the gallbladder and small intestines due to the unfavorable biliary excretion of this rather lipophilic tracer. We recently compared a series of pyrimidine nucleoside and acycloguanosine derivatives to identify an optimized tracer for monitoring HSV1-tk and HSV1-sr39tk gene expression and found that ^{3}H-2′-fluoro-2′-deoxyarabinofuranosyl-5-ethyluracil (^{3}H-FEAU) exhibited the highest or second highest uptakes regardless of the mode of transfer (stably transfected or viral mediated) of both HSV1-tk and a mutant HSV1-sr39tk (39). Whether ^{18}F-FEAU may be used to monitor Ad vector (both Adtk and RGD-PEG-Adtk) infectivity in vivo with more favorable pharmacokinetics than ^{18}F-FHBG requires further investigation.

CONCLUSION

We have successfully modified E1- and E3-deleted Ad vector carrying mutant herpes simplex virus 1 thymidine kinase (HSV1-39tk) reporter gene using heterofunctional PEG. PEGylation completely ablated the natural tropism of the virus even at a low rate of modification of the fiber knobs. The addition of monomeric cyclic RGD peptides showed enhanced transduction efficiency in those cells expressing integrin $\alpha_v\beta_3$ and was observed in both in vitro and in vivo studies. This enhancement in transduction is dependent on the binding of the coupled RGD peptide to integrin and is independent of CAR viral receptors. Non-target tissues such as liver showed a marked decrease in transduction after intravenous delivery of the modified vector, suggesting that PEGylation may help reduce the in vivo sequestration of the vector. Noninvasive PET and ^{18}F-FHBG were able to monitor in vivo transfectivity of both Adtk and RGD-PEG-Adtk vectors in the liver and tumors after intravenous injection, which correlated well with ex vivo tissue TK enzyme activity. ^{18}F-

FHBG PET appears to be appropriate to monitor chemically modified HSV1-sr39tk/ganciclovir (GCV) suicide gene therapy efficacy.

Acknowledgments

This work was supported, in part, by National Institute of Biomedical Imaging and Bioengineering grant R21 EB001785, Department of Defense (DOD) Breast Cancer Research Program (BCRP) Concept award DAMD17-03-1-0752, DOD BCRP IDEA award W81XWH-04-1-0697, DOD Ovarian Cancer Research Program award OC050120, DOD Prostate Cancer Research Program New Investigator award DAMD1717-03-1-0143, the American Lung Association California, the Society of Nuclear Medicine Education and Research Foundation, National Cancer Institute (NCI) Small Animal Imaging Resource Program grant R24 CA93862, and NCI In Vivo Cellular Molecular Imaging Center grant P50 CA114747.

References

1. Smith AE. Viral vectors in gene therapy. Annu Rev Microbiol. 1995; 49:807–838. [PubMed: 8561480]
2. Kanerva A, Hemminki A. Modified adenovirus for cancer gene therapy. Int J Cancer. 2004; 110:475–480. [PubMed: 15122578]
3. Bergelson JM, Cunningham JA, Droguett G, et al. Isolation of a common receptor for coxsackie B viruses and adenoviruses 2 and 5. Science. 1997; 275:1320–1323. [PubMed: 9036860]
4. Dechecchi MC, Melotti P, Bonizzato A, et al. Heparan sulfate glycosaminoglycans are receptors sufficient to mediate the initial binding of adenovirus types 2 and 5. J Virol. 2001; 75:8772–8780. [PubMed: 11507222]
5. Bergelson JM, Krithivas A, Celi L, et al. The murine CAR homolog is a receptor for coxsackie B viruses and adenoviruses. J Virol. 1998; 72:415–419. [PubMed: 9420240]
6. Sullivan DE, Dash S, Du H, et al. Liver-directed gene transfer in non-human primates. Hum Gene Ther. 1997; 8:1195–1206. [PubMed: 9215737]
7. Zinn KR, Douglas JT, Smyth CA, et al. Imaging and tissue biodistribution of ^{99m}Tc-labeled adenovirus knob (serotype 5). Gene Ther. 1998; 5:798–808. [PubMed: 9747460]
8. Croyle MA, Chirmule N, Zhang Y, et al. Pegylation of E1-deleted adenovirus vectors allows significant gene expression on readministration to liver. Hum Gene Ther. 2002; 13:1887–1900. [PubMed: 12396620]
9. Zabner J, Freimuth P, Puga A, et al. Lack of high affinity fiber receptor activity explains the resistance of ciliated airway epithelia to adenovirus infection. J Clin Invest. 1997; 100:1144–1149. [PubMed: 9276731]
10. Jooss K, Chirmule N. Immunity to adenovirus and adeno-associated viral vectors: implications for gene therapy. Gene Ther. 2003; 10:955–963. [PubMed: 12756416]
11. Barr D, Tubb J, Ferguson D, et al. Strain related variations in adenovirally mediated transgene xpression from mouse hepatocytes in vivo: comparisons between immunocompetent and immunodeficient inbred strains. Gene Ther. 1995; 2:151–155. [PubMed: 7719932]
12. Boucher RC. Current status of CF gene therapy. Trends Genet. 1996; 12:81–84. [PubMed: 8868343]
13. Work LM, Ritchie N, Nicklin SA, et al. Dual targeting of gene delivery by genetic modification of adenovirus serotype 5 fibers and cell-selective transcriptional control. Gene Ther. 2004; 11:1296–1300. [PubMed: 15292916]
14. Dmitriev I, Krasnykh V, Miller CR, et al. An adenovirus vector with genetically modified fibers demonstrates expanded tropism via utilization of a coxsackievirus and adenovirus receptor-independent cell entry mechanism. J Virol. 1998; 72:9706–9713. [PubMed: 9811704]
15. Reynolds PN, Dmitriev I, Curiel DT. Insertion of an RGD motif into the HI loop of adenovirus fiber protein alters the distribution of transgene expression of the systemically administered vector. Gene Ther. 1999; 6:1336–1339. [PubMed: 10455445]

16. Mok H, Palmer DJ, Ng P, et al. Evaluation of polyethylene glycol modification of first-generation and helper-dependent adenoviral vectors to reduce innate immune responses. Mol Ther. 2005; 11:66–79. [PubMed: 15585407]

17. Ogawara K, Rots MG, Kok RJ, et al. A novel strategy to modify adenovirus tropism and enhance transgene delivery to activated vascular endothelial cells in vitro and in vivo. Hum Gene Ther. 2004; 15:433–443. [PubMed: 15144574]

18. Croyle MA, Chirmule N, Zhang Y, et al. PEGylation of E1-deleted adenovirus vectors allows significant gene expression on readministration to liver. Hum Gene Ther. 2002; 13:1887–1900. [PubMed: 12396620]

19. O'Riordan CR, Lachapelle A, Delgado C, et al. PEGylation of adenovirus with retention of infectivity and protection from neutralizing antibody *in vitro* and *in vivo*. Hum Gene Ther. 1999; 10:1349–1358. [PubMed: 10365665]

20. O'Riordan CR, Song A, Lanciotti J. Strategies to adapt adenoviral vectors for targeted delivery. Methods Mol Med. 2003; 76:89–112. [PubMed: 12526160]

21. Croyle MA, Le HT, Linse KD, et al. PEGylated helper-dependent adenoviral vectors: highly efficient vectors with an enhanced safety profile. Gene Ther. 2005; 12:579–587. [PubMed: 15647765]

22. Lanciotti J, Song A, Doukas J, et al. Targeting adenoviral vectors using heterofunctional polyethylene glycol FGF2 conjugates. Mol Ther. 2003; 8:99–107. [PubMed: 12842433]

23. Fisher KD, Stallwood Y, Green NK, et al. Polymer-coated adenovirus permits efficient retargeting and evades neutralizing antibodies. Gene Ther. 2001; 8:341–348. [PubMed: 11313809]

24. Min JJ, Gambhir SS. Gene therapy progress and prospects: noninvasive imaging of gene therapy in living subjects. Gene Ther. 2004; 11:115–125. [PubMed: 14712295]

25. Tjuvajev JG, Doubrovin M, Akhurst T, et al. Comparison of radiolabeled nucleoside probes (FIAU, FHBG, and FHPG) for PET imaging of HSV1-tk gene expression. J Nucl Med. 2002; 43:1072–1083. [PubMed: 12163634]

26. Min JJ, Iyer M, Gambhir SS. Comparison of [^{18}F]FHBG and [^{14}C]FIAU for imaging of HSV1-tk reporter gene expression: adenoviral infection vs. stable transfection. Eur J Nucl Med Mol Imaging. 2003; 30:1547–1560. [PubMed: 14579096]

27. Mangner TJ, Klecker RW, Anderson L, et al. Synthesis of 2′-deoxy-2′-[^{18}F]fluoro-beta-D-arabinofuranosyl nucleosides, [^{18}F]FAU, [^{18}F]FMAU, [^{18}F]FBAU and [^{18}F]FIAU, as potential PET agents for imaging cellular proliferation: synthesis of [^{18}F]labelled FAU, FMAU, FBAU, FIAU. Nucl Med Biol. 2003; 30:215–224. [PubMed: 12745012]

28. Liang Q, Nguyen K, Satyamurthy N, et al. Monitoring adenoviral DNA delivery, using a mutant herpes simplex virus type 1 thymidine kinase gene as a PET reporter gene. Gene Ther. 2002; 9:1659–1666. [PubMed: 12457279]

29. Chen X, Park R, Shahinian AH, et al. Pharmacokinetics and tumor retention of ^{125}I-labeled RGD peptide are improved by PEGylation. Nucl Med Biol. 2004; 31:11–19. [PubMed: 14741566]

30. Hruby DE, Ball LA. Cell-free synthesis of enzymatically active vaccinia virus thymidine kinase. Virology. 1981; 113:594–601. [PubMed: 7269256]

31. Thibault G. Sodium dodecyl sulfate-stable complexes of echistatin and RGD-dependent integrins: a novel approach to study integrins. Mol Pharmacol. 2000; 58:1137–1145. [PubMed: 11040063]

32. Felding-Habermann B, O'Toole TE, Smith JW, et al. Integrin activation controls metastasis in human breast cancer. Proc Natl Acad Sci U S A. 2001; 98:1853–1858. [PubMed: 11172040]

33. Kumar CC. Integrin $\alpha_v\beta_3$ as a therapeutic target for blocking tumor-induced angiogenesis. Curr Drug Targets. 2003; 4:123–131. [PubMed: 12558065]

34. Chen X. Multimodality imaging of tumor integrin expression. Mini Rev Med Chem. In press.

35. Haubner R, Wester HJ. Radiolabeled tracers for imaging of tumor angiogenesis and evaluation of anti-angiogenic therapies. Curr Pharm Des. 2004; 10:1439–1455. [PubMed: 15134568]

36. Haubner R, Weber WA, Beer AJ, et al. Noninvasive visualization of the activated $\alpha_v\beta_3$ integrin in cancer patients by positron emission tomography and [^{18}F]galacto-RGD. PLOS Med. 2005; 2:e70. serial online. [PubMed: 15783258]

37. McConnell MJ, Imperiale MJ. Biology of adenovirus and its use as a vector for gene therapy. Hum Gene Ther. 2004; 15:1022–1033. [PubMed: 15610603]

38. Wu Y, Zhang X, Xiong Z, et al. microPET imaging of glioma integrin $\alpha_v\beta_3$ expression using ^{64}Cu-labeled tetrameric RGD peptide. J Nucl Med. 2005; 46:1707–1718. [PubMed: 16204722]

39. Kang KW, Min JJ, Chen X, Gambhir SS. Comparison of [^{14}C]FMAU, [^{3}H]FEAU, [^{14}C]FIAU, and [^{3}H]PCV for monitoring reporter gene expression of wild type and mutant herpes simplex virus type 1 thymidine kinase in cell culture. Mol Imaging Biol. Jul 23.2005 Epub ahead of print.

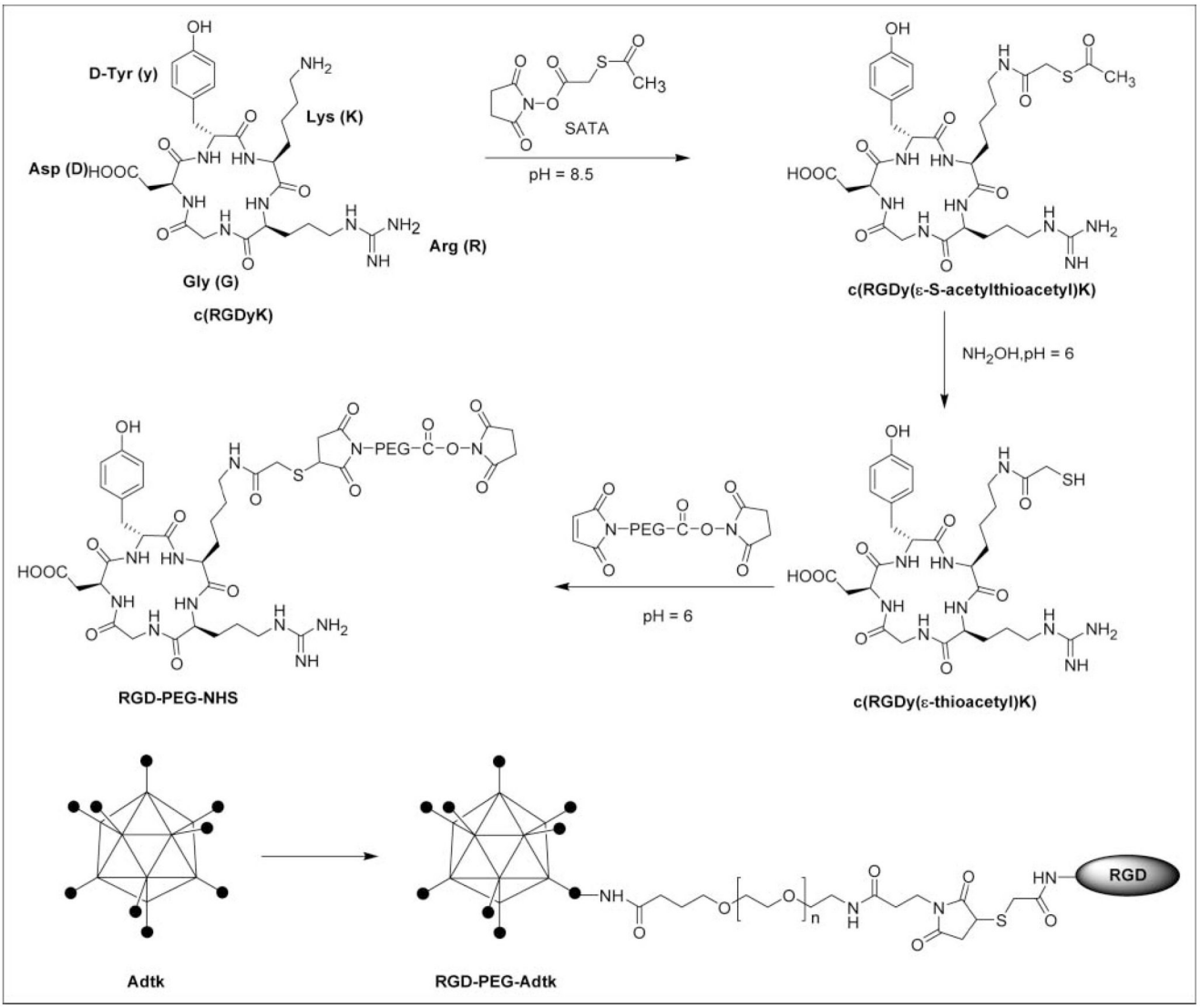

FIGURE 1.

Schematic representation of Ad vector modified with RGD-PEG. Synthesis of RGD-PEG-NHS (where NHS = *N*-hydroxysuccinimide) is shown on the top and coupling is shown on the bottom. Where Adtk is the first-generation Ad vector encoding the HSV1-sr39tk gene; RGD is a head-to-tail cyclic pentapeptide carrying arginine-glycine-aspartic acid (RGD) sequence; PEG is poly(ethylene glycol) (molecular weight, 3,400 Da) with *N*-hydroxysuccinimide ester, which reacts with primary amino groups on the adenovirus, and maleimide group, which reacts with the thiolated RGD peptide, at each end of the PEG linker.

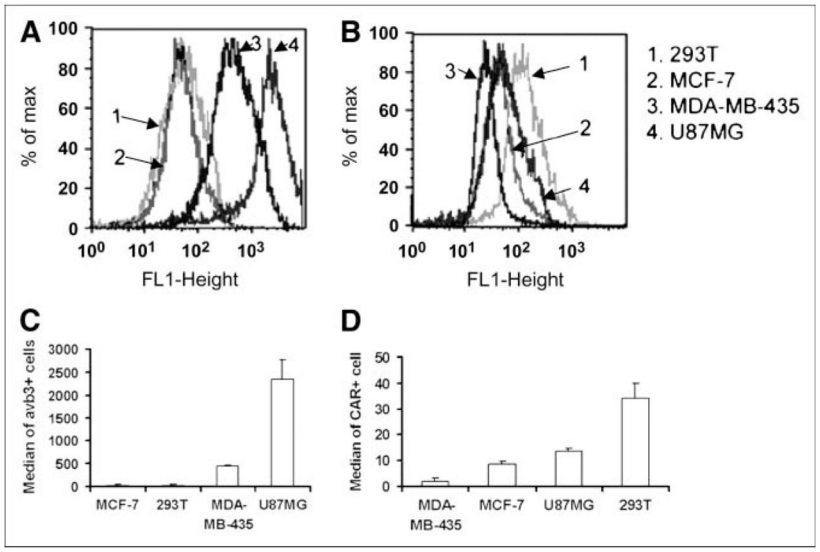

FIGURE 2.

Flow cytometric analysis of expression levels of $\alpha_v\beta_3$ integrin (A) and CAR (B) in 293T, MCF-7, U87MG, and MDA-MB-435 cells. The median of $\alpha_v\beta_3$-positive and CAR-positive cells is shown in C and D, respectively.

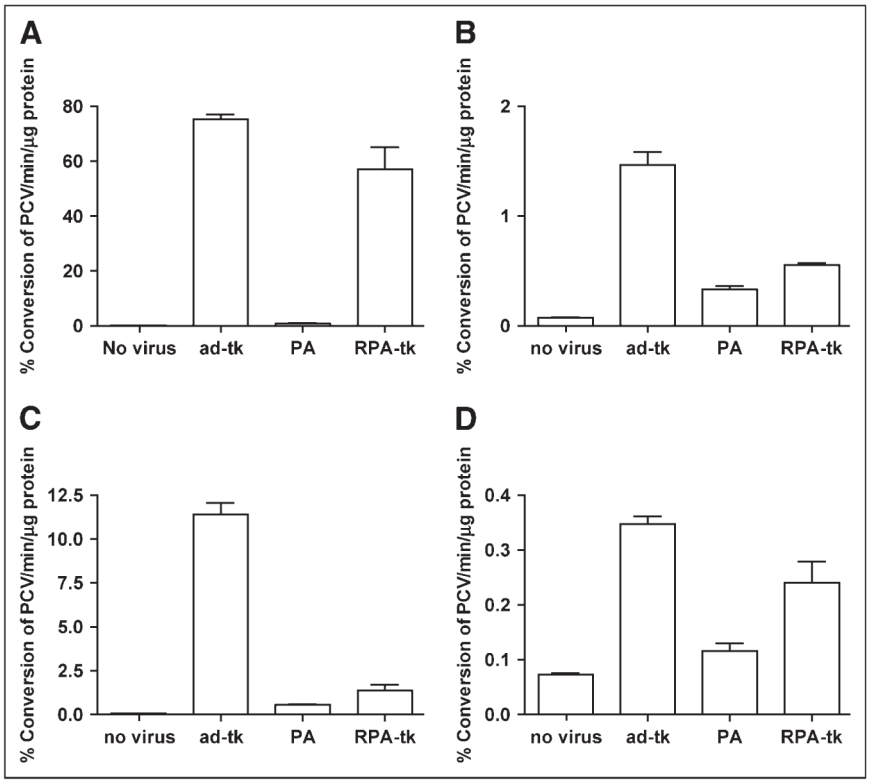

FIGURE 3.

Transduction of Adtk, PEG-Adtk, and RGD-PEG-Adtk in 293T (A), MCF-7 (B), U87MG (C), and MDA-MB-435 (D) cells. Results are expressed as the mean % conversion of ^{3}H-PCV/min/µg protein of the cell lysates ± SD. Significantly higher transduction efficiency of RGD-PEG-Adtk than that of PEG-Adtk was found in all 4 cell types. PA = PEG-Adtk.

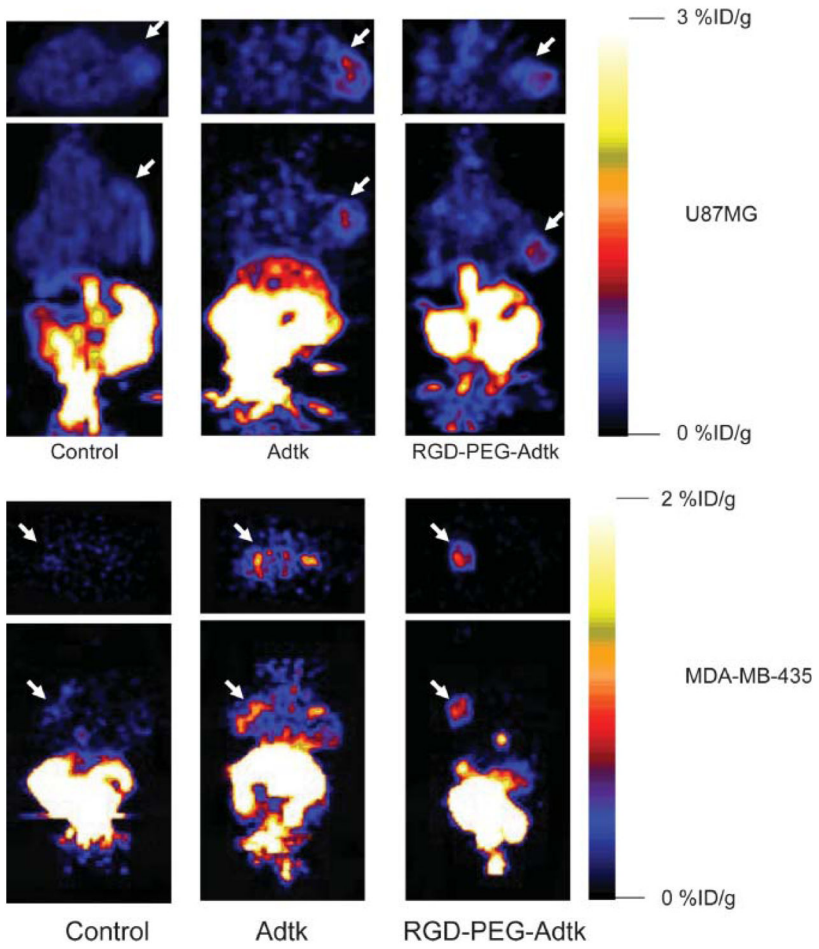

FIGURE 4.

microPET of tumor-bearing mice (top: subcutaneous U87MG tumor on right shoulder; bottom: orthotopic MDA-MB-435 tumor on left mammary fat pad) 1 h after injection of ^{18}F-FHBG (10-min static scan). Images (both trans-axial and coronal) were normalized to the same scale. The tumors are indicated by white arrows in all cases.

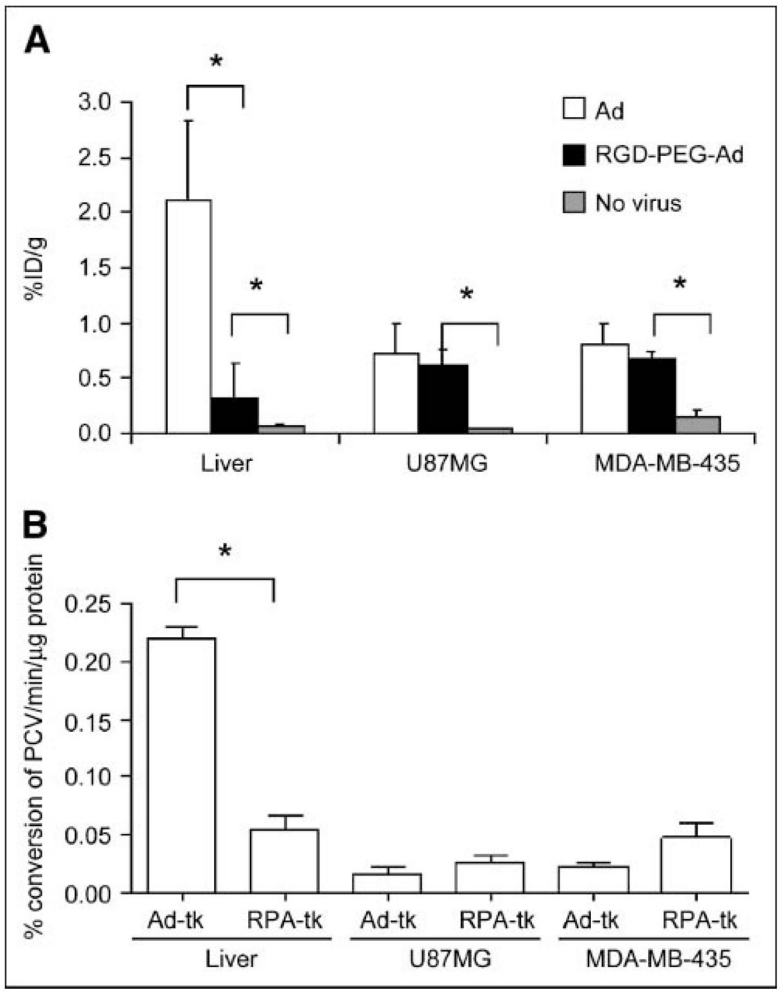

FIGURE 5.

(A) ^{18}F-FHBG retention in the form of %ID/g by measuring ROIs in organs of liver and in U87MG and MDA-MB-435 tumors after transfection of unmodified and modified Ad vectors. Data are presented as average ± SD (n = 3). Dose of virus was normalized to 20-g mouse body weight. (B) Percent conversion of ^{3}H-PCV in tissue lysates from mice after 48 h of exposure to Adtk and RGD-PEG-Adtk. *P < 0.001.

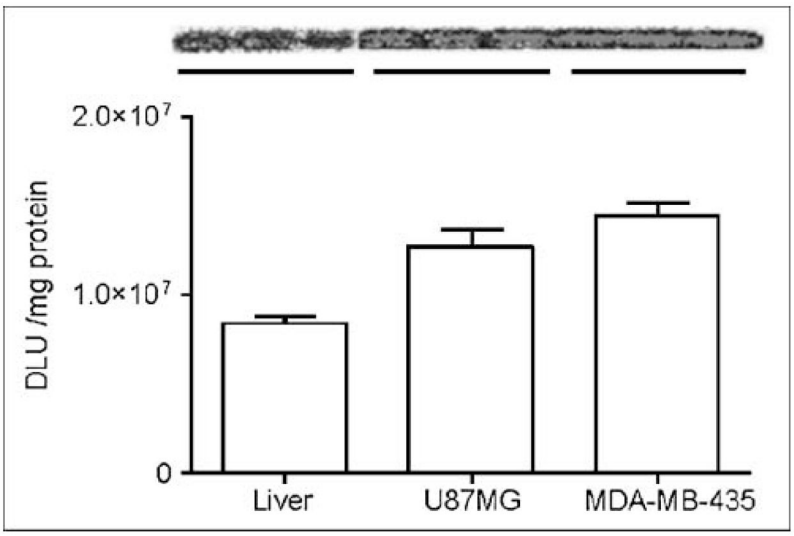

FIGURE 6.

Comparison of integrin expression in liver and in MDA-MB-435 and U87MG tumor tissue lysates by SDS-PAGE/autoradiography using ^{125}I-echistatin as $\alpha_v\beta_3$-specific radio-ligand. DLU = digital light unit.